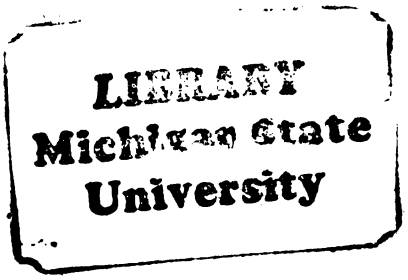

This is to certify that the

thesis entitled

MODELING OF ENZYME DEGRADATION IN
STIRRED TANKS

presented by

Michael Douglas Waite

has been accepted towards fulfillment
of the requirements for

M. S. degree in Chemical Engineering

Donald A. Anderson

Major professor

Date May 17, 1984

MODELING OF ENZYME DEGRADATION IN STIRRED TANKS

By

Michael Douglas Waite

A THESIS

Submitted to
Michigan State University
in partial fulfillment of the requirements
for the degree of

MASTER OF SCIENCE

Department of Chemical Engineering

1981

ABSTRACT

MODELING OF ENZYME DEGRADATION IN STIRRED TANKS

by

Michael Douglas Waite

Enzymes are known to lose activity when exposed to shear forces in turbulent flow systems. This thesis is an attempt to predict the deactivation of catalase in a stirred tank. The method requires that the shear dependence of the degradation kinetics be determined. The enzyme is subjected to the pure shear flow generated in a couette viscometer. Spectrophotometry is used to follow the activity loss and determine the shear degradation kinetics.

The extrapolation of the knowledge of shear inactivation in pure shear flow to a stirred tank is hindered by the lack of basic understanding of turbulence in stirred tanks. Various hypothetical models for a shear probability distribution function are proposed. Using these distribution functions and the shear degradation kinetics, rate expressions for the degradation in stirred tanks are developed.

The predictions are very sensitive to the choice of shear distribution function. A successful fit is achieved using this method with a distribution function as follows:

$$F_{(s)} = \frac{3}{\{\ln(\frac{s_{max}}{s_0})\}^3} \frac{\{-\ln(\frac{s}{s_{max}})\}^2}{s} \quad s_0 \leq s \leq s_{max}$$

$$\frac{3}{s_0^2} \frac{s}{\ln(\frac{s_{max}}{s_0})} \quad 0 \leq s \leq s_0$$

To my wife

Retha

ACKNOWLEDGMENTS

Sincere appreciation is extended to Professor Donald Anderson, who suggested this area of research, and for his support throughout the course of this work. I would like to acknowledge Dr. Carl Beck, whose enzyme studies preceded this and laid the groundwork for my research. Gratitude is also expressed to Professor Charles Petty, whose interest and suggestions were of great value.

TABLE OF CONTENTS

LIST OF TABLES

LIST OF FIGURES

NOTATION

a	enzyme activity	units/cm^3
A	constant	
B	constant	
c,C	constants	sec
C'	constant	sec^2
[e]	enzyme concentration	$\mu g/ml$
$F,F_{(s)}$	shear probability density function	sec
G	constant	
k	H_2O_2 decay reaction rate constant	$\frac{ml \cdot l}{\mu g\ mM\ sec^2}$
k'	H_2O_2 decay reaction rate constant with enzyme concentration	$\frac{1}{mM\ sec^2}$
k'_i	initial rate constant for H_2O_2 decay	$\frac{1}{mM\ sec^2}$
K_s	enzyme degradation rate constant due only to shear	min^{-1}
K_t	enzyme degradation rate constant in the stirred tank	min^{-1}
K_v	enzyme degradation rate constant in the viscometer	min^{-1}
K_{vo}	initial viscometer enzyme degradation rate constant	min^{-1}
ℓ	height of control volume for Model 5	cm
m	constant	
n	order of enzyme degradation reaction with respect to shear rate	
N	speed of outer cylinder	min^{-1}

P	power input to tank	erg/sec
Q	geometrical constant	
r	radius of control volume for Model 5	cm
r_g	radial position within the viscometer gap	cm
R_o	inner radius of outer cylinder	cm
R_s	rate of enzyme degradation due only to shear	$\frac{\text{activity}}{\text{cm}^3\ \text{sec}}$
R_t	rate of enzyme degradation in tank	$\frac{\text{activity}}{\text{cm}^3\ \text{sec}}$
R_v	rate of enzyme degradation in the viscometer	$\frac{\text{activity}}{\text{cm}^3\ \text{sec}}$
R_{vo}	initial viscometer degradation rate	$\frac{\text{activity}}{\text{cm}^3\ \text{sec}}$
s	shear rate	sec^{-1}
$[S]$	substrate concentration	mM
$[S_i]$	initial substrate concentration	mM
$\langle s \rangle$	mean shear rate	sec^{-1}
$\langle s^2 \rangle$	variance in shear rate	sec^{-2}
s_{max}	maximum shear rate	sec^{-1}
s_o	intermediate shear rate	sec^{-1}
t	time of assay	sec
Tq	torque	erg
v	control volume for Model 5	cm^3
V	tank volume	cm^3
Z	proportionality constant	$\frac{\text{sec}}{\text{min}}$

GREEK SYMBOLS

θ	shear exposure time	min
μ	viscosity	poise
Γ	gamma function	
Ω	angular velocity	radians/sec

INTRODUCTION

Enzymes are high molecular weight proteins that exhibit biological catalytic activity. As catalysts they are remarkable, often accelerating reactions by a factor of 10^8 to 10^{10}. The extremely complex three dimensional structure of enzymes is necessary for their effectiveness and specificity. The conformation of enzymes is unique to each species and depends upon the peptide bond "backbone" and the interaction of hydrogen bonds and van der Waal's forces acting as cross members. Enzyme structure can be effected by pH, temperature, chemical inactivators, microbial contaminants or mechanical forces induced by shear or possibly elongational flow fields.

The peptide bonds are resistant to cleavage, and are prevented from rotating by the hydrogen bonds and van der Waal's forces. These weaker bonds can dissociate more easily resulting in a loss of catalytic activity or even denaturation (unraveling). Although enzymes are fragile, renaturation and a renewal of activity is possible and often rapid so that only those enzymes which have been irreparably damaged contribute to the loss of activity.

A number of industrial applications have been found for enzymes but permanent degradation of the active site prevents exploitation of many potentially beneficial enzymes. The deactivation of enzymes in a shear field would be unavoidable in any large-scale chemical process since all mixing or pumping operations involve shear forces.

The problem has been studied by a number of investigators. Much of this work concerned immobilized enzymes used in fluidized or fixed bed reactors (6, 14, 15). There are many commercial applications that might require the use of free enzymes in solution such as in the conversion of cellulose to glucose, production of some pharmaceuticals, or in the removal of hydrogen peroxide from milk during cheese processing (16).

One of the first investigations of shear deactivation of free enzymes was performed by Charm and Wong (7). The authors reported activity losses for the enzymes rennet, catalase, and carboxy peptidase when exposed to known shear rates in a couette viscometer. Additional work was completed by this group in which different flow systems were examined and activity loss was predicted based on the known response to the pure shear field (9).

Studies by Tirrell (19, 20, 21) modeled the degradation of urease and lactic dehydrogenase using the shear stress rather than shear rate. Work by Beck (3) attempted to predict the response of the enzyme catalase to the turbulent

shear experienced in a standard stirred tank. Couette viscometer data provided information about the rate of degradation in a pure shear field.

This study will attempt to validate the proposed rate expression,

$$R_s = K_s a \qquad 1$$

where,

$$K_s = Z s^n \qquad 2$$

R_s is the rate of enzyme inactivation in a shear field, K_s is the enzyme degradation reaction rate constant, s is the shear rate, and n is an unknown constant. These expressions imply that an enzyme solution exposed to a constant shear field will lose activity at a rate proportional to the concentration of active enzyme. The rate constant is a function of the shear rate and a plot of $\ln(K_s)$ vs. $\ln(s)$ gives the order on the shear rate n, as well as the constant of proportionality Z.

It would be useful to be able to extrapolate knowledge about shear inactivation in a couette apparatus to stirred tanks or other equipment with unknown shear structures. Various hypothetical models for the distribution of shear rate magnitudes are proposed here for stirred tanks and are tested against experimentally determined deactivation rates. For an arbitrary shear distribution function the rate of degradation in a tank is given by

$$R_t = \int R_s F_{(s)} ds \qquad 3$$

where $F_{(s)}$ is the shear probability density function. The integration is performed over the domain of $F_{(s)}$, and results in an enzyme degradation rate expression. It is proposed that one (unknown) parameter can be evaluated in terms of the rate of energy dissipation for shear flow given by

$$\frac{dP}{dV} = \mu s^2 \qquad 4$$

where μ is the viscosity of the fluid and P is the power input. The final rate expression is of the form

$$R_t = G \frac{Z}{\mu^{\frac{1}{2}}} \left(\frac{P}{V}\right)^{\frac{1}{2}} a \qquad 5$$

where G is a dimensionless constant and the enzyme degradation rate constant in the tank is given by

$$K_t = G \frac{Z}{\mu^{\frac{1}{2}}} \left(\frac{P}{V}\right)^{\frac{1}{2}} \qquad 6$$

Each of the proposed rate expressions are checked against degradation rate data taken from the stirred tank.

BACKGROUND

Enzymes are polymers of the α-amino acids. They demonstrate biological catalytic activity and are essential to all life forms. The most common unit of enzyme activity is defined as the amount of enzyme which causes transformation of one micromole of substrate per minute at 25°C under optimal conditions of measurement. The catalytic ability of some enzymes is given in Table 1 (11).

Table 1. Molecular activity given in moles of substrate transformed per mole of enzyme per minute under optimal conditions

Enzyme	Activity
Carbonic Anhydrase C	36,000,000
Catalase	5,600,000
β Amylase	1,100,000
β Galactosidase	12,500
Phosphoglucomutase	1,240
Succinate Dehydrogenase	1,150

The great activity of enzymes is the result of a highly refined structure which has four major levels. Primary structure refers to the covalent linkage and sequence of the amino acid backbone. The amino acid residues are bound head to tail by peptide bonds. Secondary structure refers to the recurring arrangement in space of the polypeptide

chain along one dimension. These chains may have a longitudinally coiled or extended conformation. Tertiary structure refers to the folding or bending of the polypeptide chain in three dimensions to form the compact structure of the globular protein. Quarternary structure refers to the arrangement of chains in relation to one another. Typical large proteins contain two or more polypeptide chains or subunits which are not covalently linked.

In addition to the covalently bound sequence of amino acids, the effects of hydrogen bonding, van der Waal's forces, electrostatic forces, hydrophobic forces, and intramolecular covalent crosslinks also play an important role in the native conformation of a protein molecule. This structure is almost always identical in every molecule of that protein. Enzymes or other proteins whose function involves binding small molecules, have as an essential part of their structure an "active site". The ultimate purpose of the three dimensional form of enzymes is to generate these active sites so that those groups responsible for binding and catalysis are appropiately positioned.

Obviously, there is considerable interest in exploiting the catalytic properties of enzymes. Many commercial processes currently use enzymes and many more processes which require moderate to extreme conditions of temperature, pressure, pH, etc. could become increasingly economical. Several notable examples of the practical uses of enzymes are listed in Table 2 (16).

Table 2. Commercial Uses of Enzymes

Enzyme	Typical Uses
α-Amylase	Textile desizing; starch liquefaction; glucose production.
Invertase	Production of confections such as soft-center candies.
Pectic enzymes	Clarification of fruit juices and wines.
Celluloses	Digestive aid; reduction of viscosity of vegetable gums such as those in coffee.
Bromelain	Digestive aid; anti-inflammatory preparations; meat tenderizer.
Papain	Meat tenderizer; chill proofing beer.
Trypsin	Digestive aid; leather bating.
Rennins	Curdle milk in cheese formation.
Lipases	Digestive aid; waste disposal; alter flavors by modifying milk fats.
Pancreatin	Digestive aid.
Glucose oxidase	Removal of oxygen from food products; desugars eggs; diagnostic aid (glucose in diabetes).
Catalase	Removal of hydrogen peroxide when used for sterilization, especially in milk.
Glucose isomerase	Production of high-fructose corn syrups.

The enzyme used in this study is bovine liver catalase. It is a globular protein classified as a metaloenzyme with a molecular weight of approximately 250,000. Catalase is high in sulfhydryl groups and has extensive areas of hydrophobic random coil. Its high molecular weight and chemical properties are believed to be responsible for the relative sensitivity to shear modification.

Catalase has a distinctive absorption spectrum due to the presence of an iron-porphyrin prosthetic group as part of the active site. Upon mixing with the substrate hydrogen peroxide, catalase exhibits a transient change in absorption characteristics reflecting the formation and decomposition of an enzyme-substrate complex (2). It is believed that the free iron ligand bonds the hydrogen peroxide directly as a prelude to catalysis.

EQUIPMENT

A. Viscometer

The shear field generator used in this study was constructed by Beck (3), Figure 1. A couette viscometer is capable of shearing a relatively large amount of fluid and is readily modeled. The outer cylinder is rotated at a constant rate while the inner cylinder is stationary and acts as a heat sink for the sheared fluid.

The shear rate experienced by any differential volume of fluid in the viscometer is a function of radial position r_g, and turning rate of the outer cylinder in revolutions per minute N. Shear is a maximum at the outer wall and decreases to a minimum at the inner wall. Since the gap is very narrow, the shear rate is nearly constant throughout the fluid. An average shear rate $\bar{s}_{(N)}$, can be found by integrating the shear for any differential volume over the radial position and dividing by the average radius. In cylindrical coordinants this becomes

$$\bar{s}_{(N)} = \frac{\int s_{(r,N)} r_g dr}{\int r_g dr_g} \qquad 7$$

An expression for $s_{(r,N)}$ can be obtained from the equation of motion (4).

$$s_{(r,N)} = 2 \frac{\pi N}{30} \frac{R_0^2}{r_g^2} \frac{Q^2}{1-Q^2} \qquad 8$$

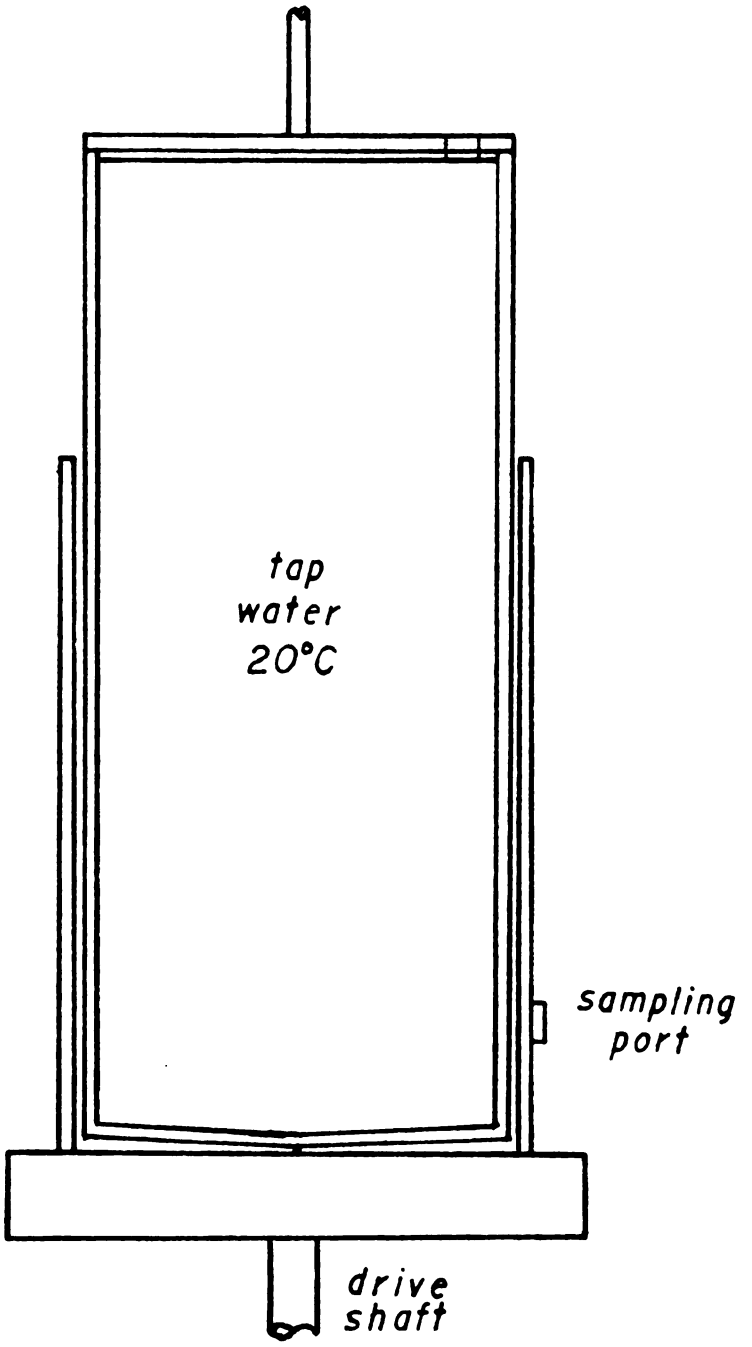

FIGURE 1. Schematic of the Coaxial Cylinder Couette Viscometer. Scale is ½, Q=0.9865

where the quantity ($\pi N/30$) is the angular velocity in reciprocal seconds, R_0 is the inner diameter of the outer cylinder, and Q is the ratio of inner gap wall radius to outer gap wall radius.

The average shear rate can be expressed as

$$\bar{s}_{(N)} = \frac{\int_{QR_0}^{R_0} 2 \frac{\pi N}{30} \left(\frac{R_0}{R_g}\right)^2 \frac{Q^2}{1-Q^2}}{\int_{QR_0}^{R_0} r_g dr_g} \qquad 9$$

Integration gives,

$$\bar{s}_{(N)} = 6.859\ N\ (sec^{-1})$$

Thus the average shear rate within the viscometer can be determined directly from the known speed of the outer cylinder.

B. Stirred Tank

A schematic diagram of the stirred tank appears in Figure 2. The tank is made of stainless steel and is industrially standardized with geometrical relationships as follows (10).

- Four baffles are used, one twelfth the tank diameter in width
- Fluid depth equals tank diameter
- A radially discharging six blade turbine is used

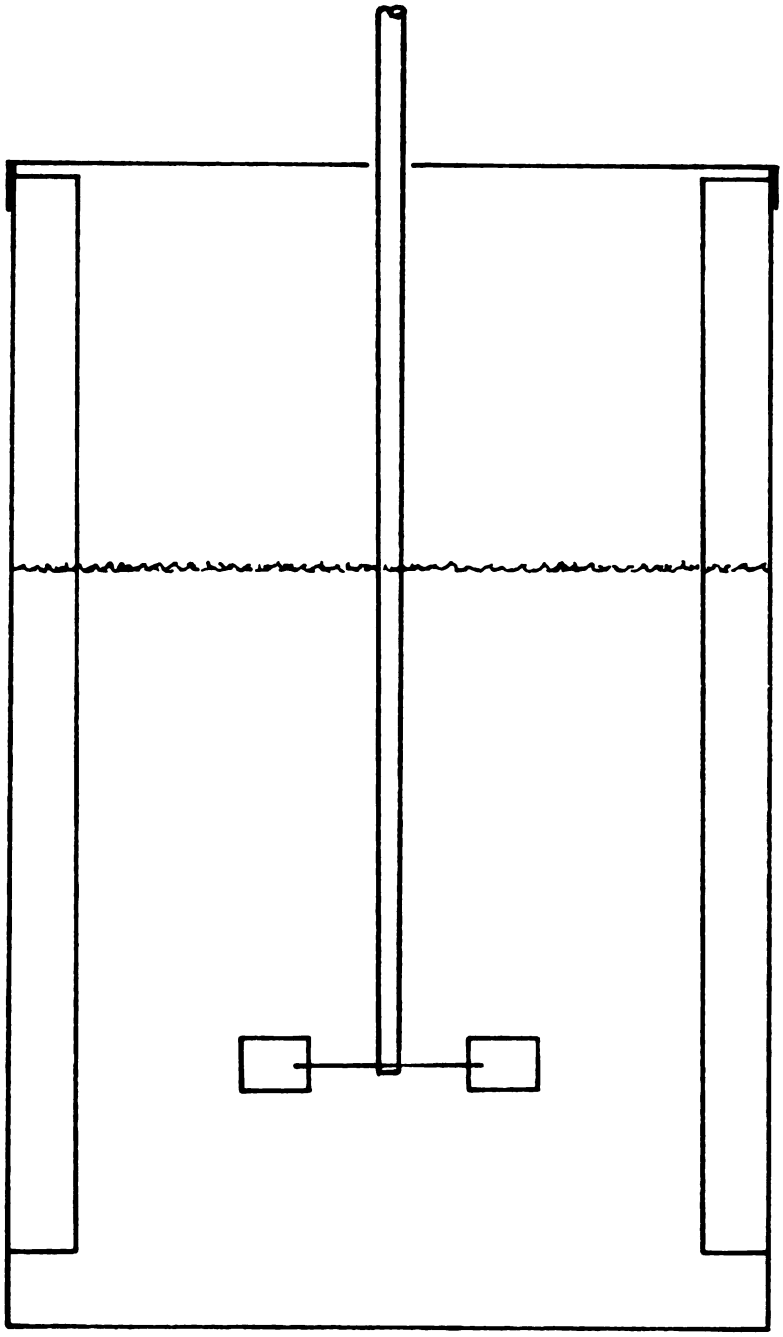

FIGURE 2. Schematic of the Stirred Tank Dimensions are specified in the Appendix.

- Impeller diameter is one third the tank diameter
- Impeller is located one third of the tank diameter from the bottom
- Impeller blade width is one fifth of the impeller diameter
- Impeller height is one fourth of impeller diameter

The temperature of the apparatus was maintained at twenty degrees centigrade with a constant temperature room. At high impeller speeds, the heat generated by viscous dissipation required the use of an external constant temperature bath.

Due to the turbulence within the tank, a drive system with good speed stability characteristics was required. A Master Controller Servodyne Drive System was used for this purpose. The motor-generator provides the impeller torque and a feedback signal to the controller which is compared to a reference. The controller then adjusts the power to the motor windings to maintain a constant output of speed. This system provides a check on the torque measurements as well as a constant impeller speed.

A dynamometer was used to measure the power input. The product of the torque arm radius and the force measured with a known mass is the torque transferred to the wall of the tank through the fluid by the impeller. The power input per unit volume is

$$\frac{P}{V} = \frac{Tq\Omega}{V} \qquad 10$$

where Ω is the angular velocity and Tq is the measured torque. Measurements of torque vs. impeller speed in revolutions per minute were taken and appear in the results section.

EXPERIMENTAL METHOD

A. Assay Method

Catalase from Worthington Biochemical Corporation (code CTS) was used in this study. The reaction of interest is the breakdown of hydrogen peroxide to form water and oxygen gas.

$$H_2O_{2(aq)} \rightarrow H_2O_{(\ell)} + \tfrac{1}{2} O_{2(g)} \quad . \qquad 11$$

According to Maehly and Chance (13), the rate expression is

$$\frac{-d[S]}{dt} = k\,[e]\,[S] \qquad 12$$

where [S] is the hydrogen peroxide concentration and k is the rate constant. Since the enzyme concentration [e] is constant during the reaction, it may be included in the rate constant to give a pseudo first order expression,

$$\frac{-d[S]}{dt} = k'[S] \qquad 13$$

Integration of the above gives

$$\ln \frac{[S]}{[S_i]} = -k't \qquad 14$$

The rate constant k' is found by plotting values of -ln ($[S]/[S_i]$) vs. time for ten second intervals. The slope of this line gives k'.

It was found that the plot of $\ln([S]/[S_i])$ vs. time is not linear which contradicts the pseudo first order rate assumption, see Figure 3. A small change in the absorbance of the enzyme upon shearing might be partially responsible. In addition, the evolution of gaseous oxygen results in bubble formation within the sample cuvette. As the reaction proceeds, the scattering effect of the accumulating bubbles could contribute to an inaccurate absorbance reading and an apparent decline in k'.

The decay of hydrogen peroxide is followed with time spectrophotometrically using a Beckman DK-2A double-beam spectrophotometer. As the reaction proceeds, the absorbance decreases in proportion to the concentration of hydrogen peroxide remaining.

The ultimate goal of the assay procedure is to determine the rate of change in enzyme activity with exposure time in the stirred tank or viscometer. Since the value of k' is proportional to the enzyme activity or the fraction of still viable enzyme molecules, the rate of enzyme degradation in a shear field can be followed during an experiment by periodically assaying for k'. The relative change in k' is all that is required. For this reason, a best straight line is used to characterize the raw data of absorbance vs. time to obtain k'.

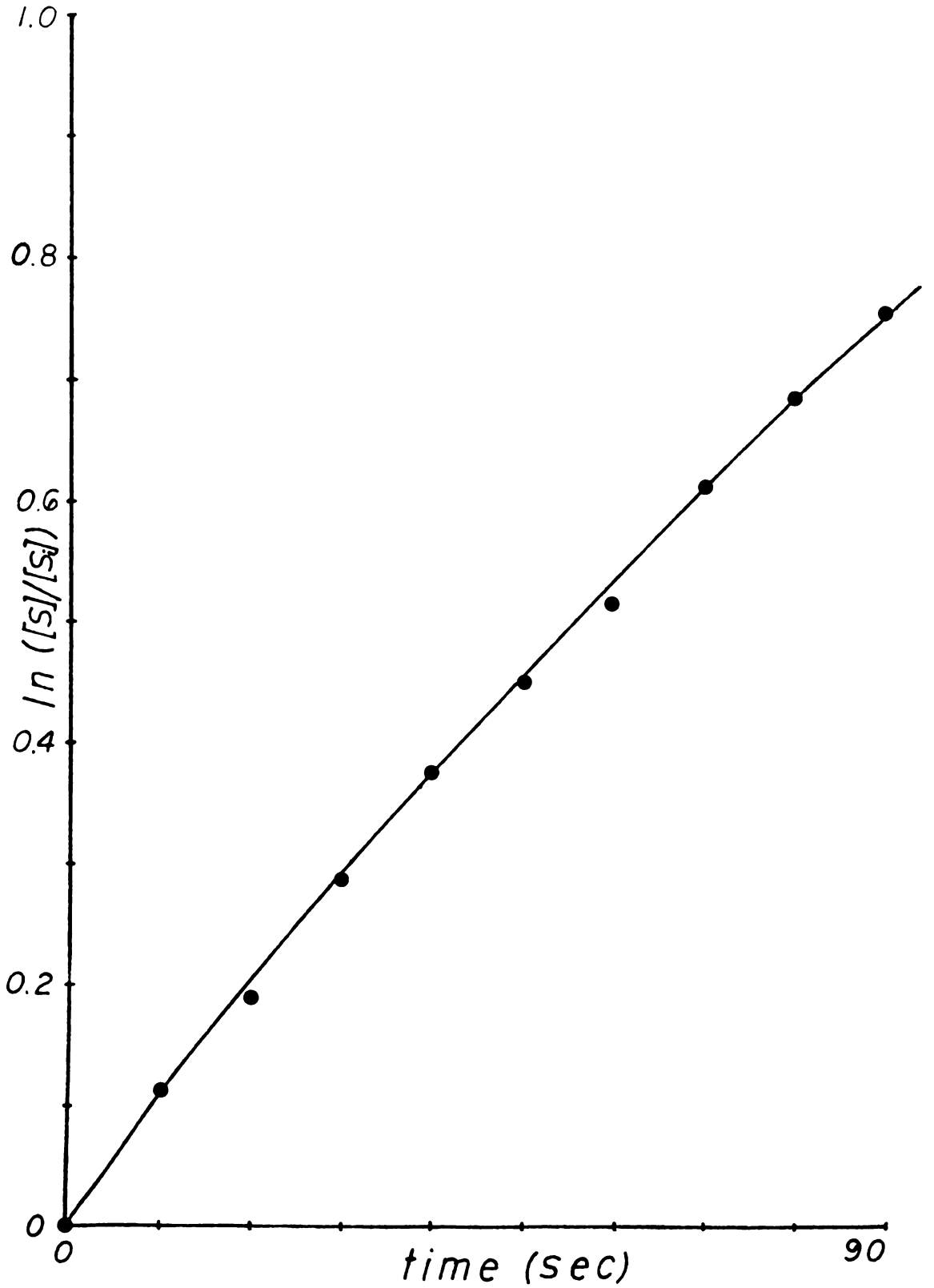

FIGURE 3. -ln ([S]/[S_i]) Versus Time for the Breakdown of Hydrogen Peroxide. Stirred tank at 1000 rpm. Exposure time is 135 minutes.

B. Procedure

Various concentrations of buffered hydrogen peroxide solution were placed in the sample cuvette and compared to a hydrogen peroxide free buffer solution to determine the most functional level of absorbance. Very high concentrations resulted in absorbance readings above 100% and excessively rapid bubble formation upon introduction of the enzyme. Low concentrations lead to very low absorbance readings and poor sensitivity to activity loss. It was found that a concentration of twenty millimolar was most useful for the substrate.

A number of trial assays were run at different catalase concentrations to confirm that the rate of hydrogen peroxide breakdown is independent of enzyme concentration. It was important to determine that the rate of hydrogen peroxide decay does not become limited by the declining enzyme concentration due to the gradual degradation in the shearing devices. A concentration of 10 µg/ml catalase was considered adequate for the enzyme.

Into one cuvette, three ml of a fifty mM potassium phosphate buffer and a ten µg/ml catalase solution is pipetted. The intermediates of the hydrogen peroxide decay are electron rich. The buffer acts as an electron acceptor stabilizing the pH at 7.0 (13). This serves as the reference cell. The sample cuvette contains three ml of a

solution that is 50 mM with respect to the buffer and 20 mM in the substrate. The spectrophotometer is equipped with a controlled temperature cell holder. The temperature is allowed to stabilize at 25° C before the cuvettes are inserted.

The spectrophotometer is then started and allowed warm up time. The output is a zero to ten mV D.C. signal which is proportional to absorbance. The recorder arm is calibrated from zero to one hundred and absorbance is read from it directly. A spectral scan of hydrogen peroxide shows that it absorbs most strongly at 2400 angstroms. Therefore, all assays are run at this wavelength to insure maximum sensitivity to deactivation.

Both the viscometer and stirred tank are equipped with sampling ports through which a 0.1 ml aliquot is extracted with a syringe. At time zero, the aliquot is injected directly into the sample cuvette. The initial absorbance reading is noted, and at 10 second intervals, an additional reading is taken until 90 seconds have elapsed. Rapid injection of the aliquot is required to assure complete mixing in a short time. Improper mixing causes erratic absorbance readings and results in missed points.

After each run, the sample cuvette is removed and rinsed thoroughly with distilled water before reuse. The cuvettes are stored in 70% nitric acid in water. This prevents accumulation of contaminants from the air or smudges which can cause inaccurate readings.

Due to the high surface to volume ratio of the viscometer, a neutral protein is added to reduce the effect of catalase adsorption to the stainless steel walls. As shown by Beck (3) albumin can be used at a concentration ten times greater than the catalase to preferentially adsorb to the viscometer. The solution used in the viscometer is prepared with,

- 0.839 ml catalase concentrate (0.835 $\frac{mg}{ml}$)
- 243 mg K_2HPO_4 (dibasic)
- 70 mg albumin (crystalline)
- Distilled water to make 70 ml total

The viscometer is set up as described in the equipment section and the inner cylinder is filled with tap water at 20^{o} C.

The stirred tank has a much lower surface to volume ratio and very little adsorption is detected. Hence, albumin is not added and the tank solution is made by mixing,

- 23.25 g K_2HPO_4
- 80.0 ml enzyme concentrate
- Distilled water to make 6670 ml total

Several assays are taken immediately after the solutions are made up to establish an initial enzyme activity. The shearing devices are then started and a predetermined routine of periodic assays is begun. Early assays are performed at five minute intervals for the first 15-20 minutes, then at 30 minute intervals for the next 3 to 5

hours. For each assay, the time of day, length of exposure to shear and the raw data (absorbance vs. time in seconds) are noted. Each shear rate in the viscometer, or impeller speed in the stirred tank, requires ten to twenty assays for the determination of the degradation rate constant K_s or K_t.

EXPERIMENTAL RESULTS

A. Viscometer Data

The raw data generated by assays on the viscometer contents shows a decreasing enzyme activity with time. The activity of the enzyme solution is proportional to the rate constant for the breakdown of hydrogen peroxide (k'). A table of k' vs. exposure time is shown in the appendix for each shear rate used. A plot of the logarithm of k'/k'_i versus exposure time generates an overall Catalase degradation rate constant in the viscometer K_v.

For a batch reaction system,

$$R_v = -\frac{da}{dt} \qquad 15$$

where the rate of enzyme deactivation in the viscometer R_v is defined as the rate of activity change with time. The viscometer rate expression is given by,

$$R_v = K_v a \qquad 16$$

where a is proportional to k'. Thus,

$$R_v = -\frac{dk'}{dt} = K_v k' \qquad 17$$

integration gives

$$-\ln\left(\frac{k'}{k'_i}\right) = K_v t \qquad 18$$

A plot of the logarithm of $\frac{k'}{k'_i}$ versus exposure time generates the overall catalase degradation rate constant in the viscometer K_v. A sample plot appears in Figure 4.

For each shear rate used, a value for K_v is determined. Table 3 lists these results. Notice that there is an intrinsic rate of degradation in the absence of shear (K_{vo}). This implies that the degradation rate constant due only to shear can be expressed as

$$K_s = K_v - K_{vo}$$

The existence of a nonzero rate constant at zero shear (K_{vo}) is a result of a number of factors. Although albumin was added to adhere to the viscometer, some residual binding is to be expected. Previous work on the same viscometer (3) showed this effect to be minimal and partially reversible upon shearing. A number of investigators have shown that catalase deactivation is accelerated by free ions of iron. It is believed that this iron is bound rather strongly to the porphyrin ring which is central to the active site of catalase (11). A further explanation is that the natural random bond breakages typically found with thermal degradation have been accelerated. Stored at room temperature, catalase has been shown to degrade up to 20% in 48 hours (8). The zero-shear degradation phenomenon does not appear to be affected by the presence of shear, and consequently can be eliminated by difference.

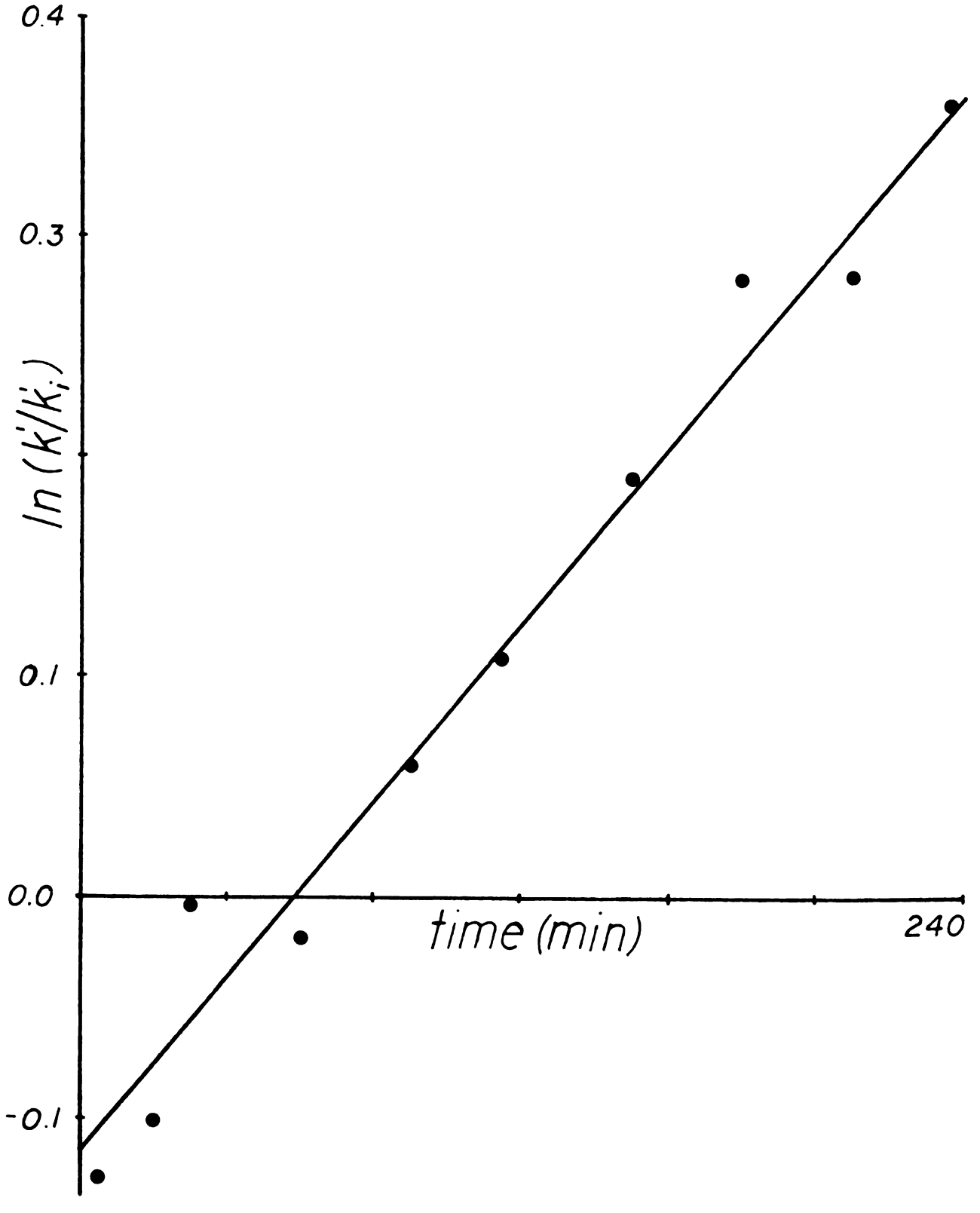

FIGURE 4. -ln (k'/k'i) Versus Exposure Time in the Viscometer. Shear rate is 1715 sec^{-1}.

Table 3. K_v vs. shear rate.

shear rate (sec^{-1})	K_v (min^{-1})
0	0.001027
643	0.001310
1286	0.001390
2572	0.001860
3835	0.002227

Table 4. K_t vs. $(P/V)^{\frac{1}{2}}$

$(P/V)^{\frac{1}{2}}$ $(g/cm\ sec^2)^{\frac{1}{2}}$	K_v (min^{-1})
0	0.000214
676	0.000947
1816	0.001410
1816	0.001633
2989	0.002640
2989	0.001985
3603	0.003097
4226	0.004060
4226	0.003439

The degradation rate constant is a function of s as shown in equation 19.

$$K_s = Zs^n \qquad 19$$

The order n and the proportionality Z can be calculated from the couette data by plotting $\ell n\ (K_s)$ vs. $\ell n\ (s)$. Figure 5 shows this plot and the values for n and Z.

B. Stirred Tank Data

Like the viscometer data, the results of the assay procedure provide a relationship between the enzyme degradation rate constant in the tank K_t, and the measured quanity $(P/V)^{\frac{1}{2}}$. This result is summarized in Table 4.

As will be shown, predictions of K_t take the form

$$K_t = G \frac{Z}{\mu^{\frac{1}{2}}} (P/V)^{\frac{1}{2}} \qquad 20$$

Since Z is known from the couette data and the viscosity μ is assumed to be essentially that of water, the stirred tank data can be used to calculate the actual value of the numerical factor G.

An important aspect of these results is that the form of the predicted rates is consistent with the data, that is, both the predicted and measured degradation rates are proportional to $(P/V)^{\frac{1}{2}}$. This finding could be useful in the scale-up of enzyme processing equipment. A geometrically similar tank one fifteenth as large was used by Beck (3) and showed a rate proportional to $(P/V)^{\frac{1}{2}}$. Figure 6 also

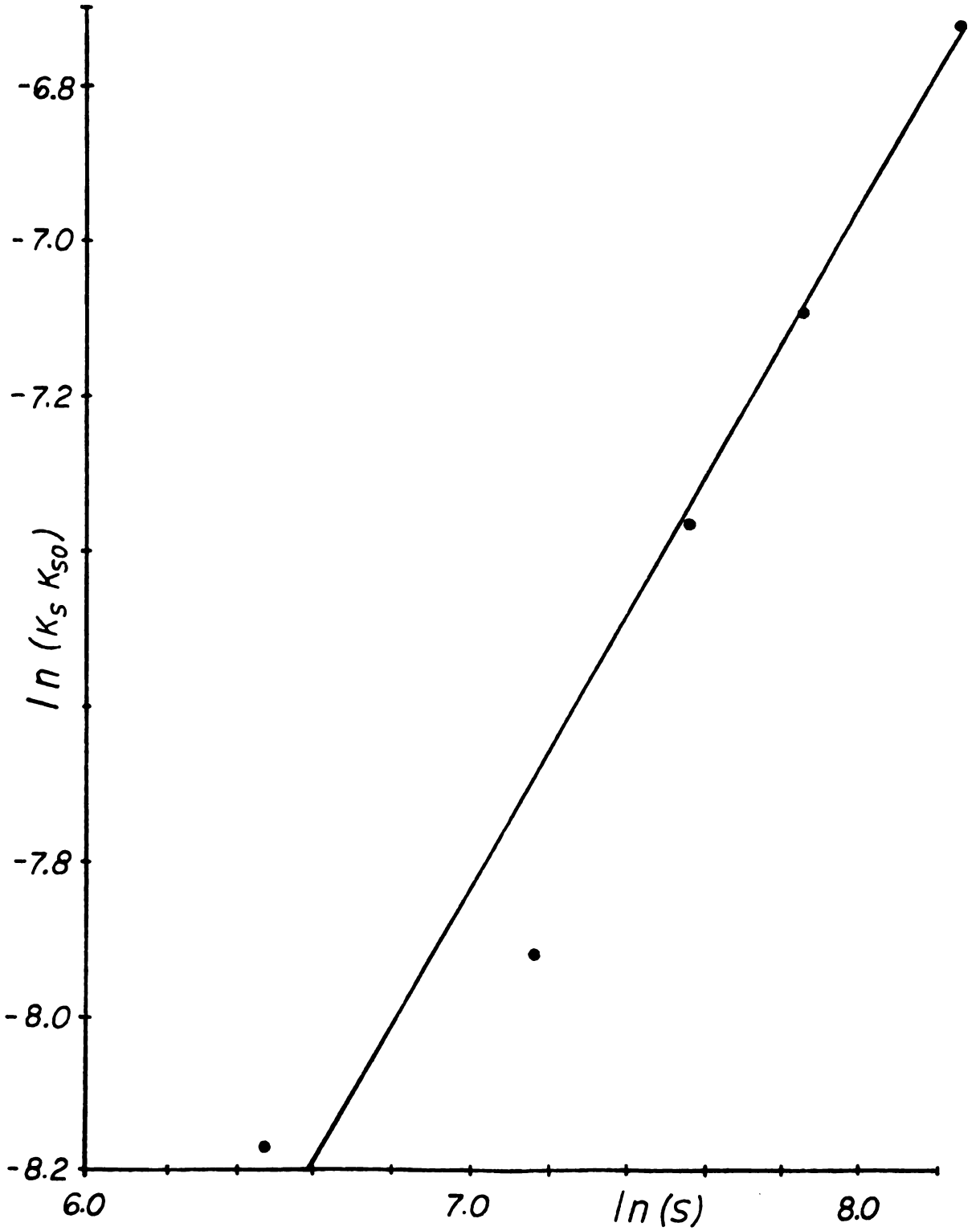

FIGURE 5. $\ln(K_s - K_{so})$ vs. $\ln(s)$ in the viscometer. The value of n is 0.041 and Z is 1.084×10^{-6} sec/min.

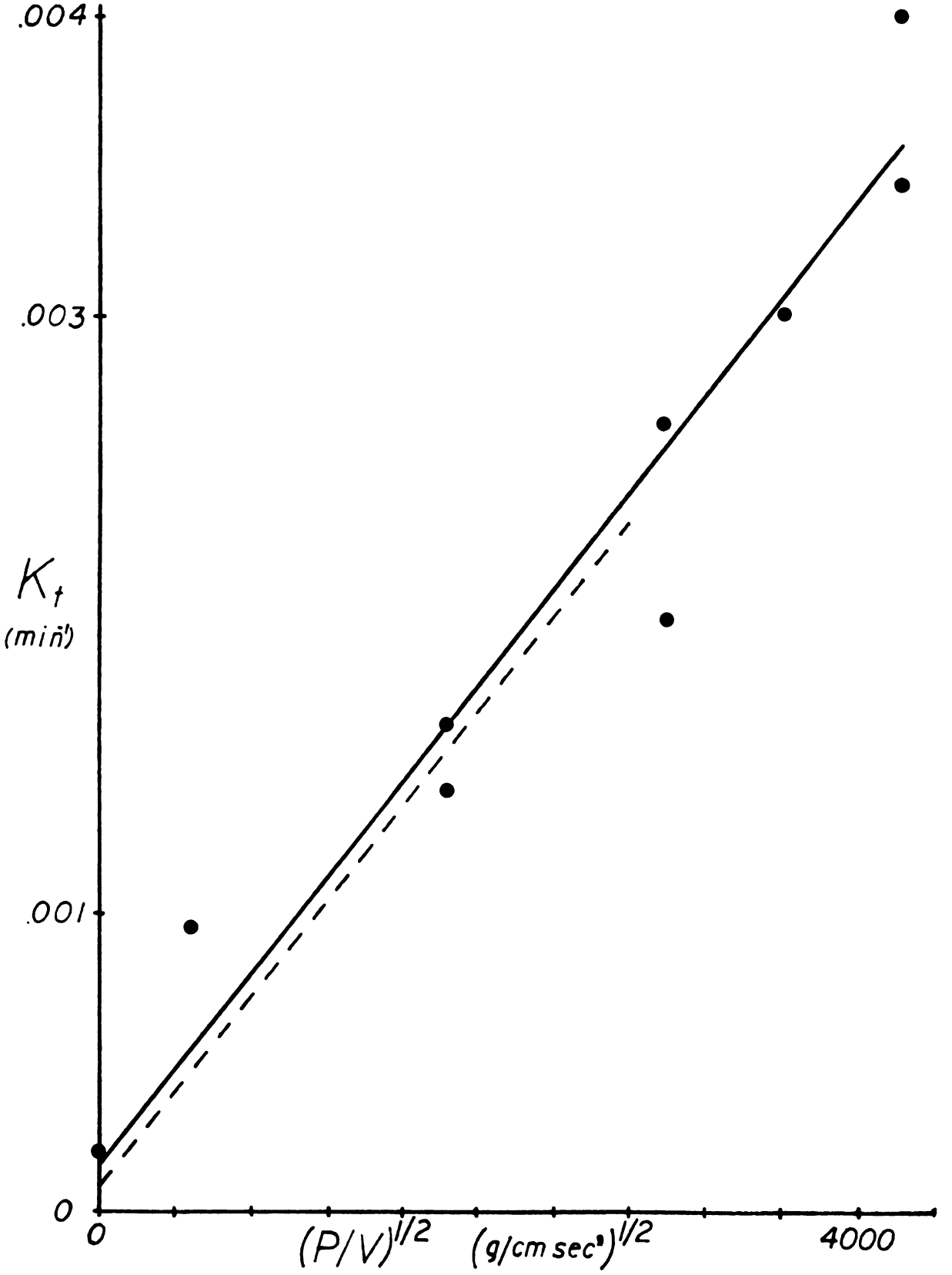

FIGURE 6. K_t Versus $(P/V)^{\frac{1}{2}}$. Slope is 8.05×10^{-7}. Dotted line: from data collected by Beck.

shows K_t vs. $(P/V)^{\frac{1}{2}}$ for the smaller tank (dotted line). As can be seen, the slopes of the lines are nearly equal. For the reasons discussed earlier, there is an intrinsic rate of degradation at zero shear which results in a positive value for the intercept. Although the intercept varies between the two tanks, this is believed to be caused by the presence of a higher dissolved mineral content in the water used in the large tank and not by a difference in volume or fluid flow patterns. The evidence strongly suggests that the power per volume would be a useful scale-up criterion for geometrically similar stirred tank enzyme reactors.

To determine the power input, the torque must be measured. The product of torque and the rate of angular displacement gives the total power input. The torque transferred to the tank wall was measured for different impeller speeds. The results appear in Figure 7 and are tabulated in the appendix.

C. Improved Activity at Short Exposure Times

An interesting result of the work in both the viscometer and the stirred tank was the commonly noticeable increase in activity found for short shearing times. This evidence compliments studies on the enzyme lactic dehydrogenase in which this phenomena is discribed as shear induced deagglomeration of groups of distinct enzyme molecules which

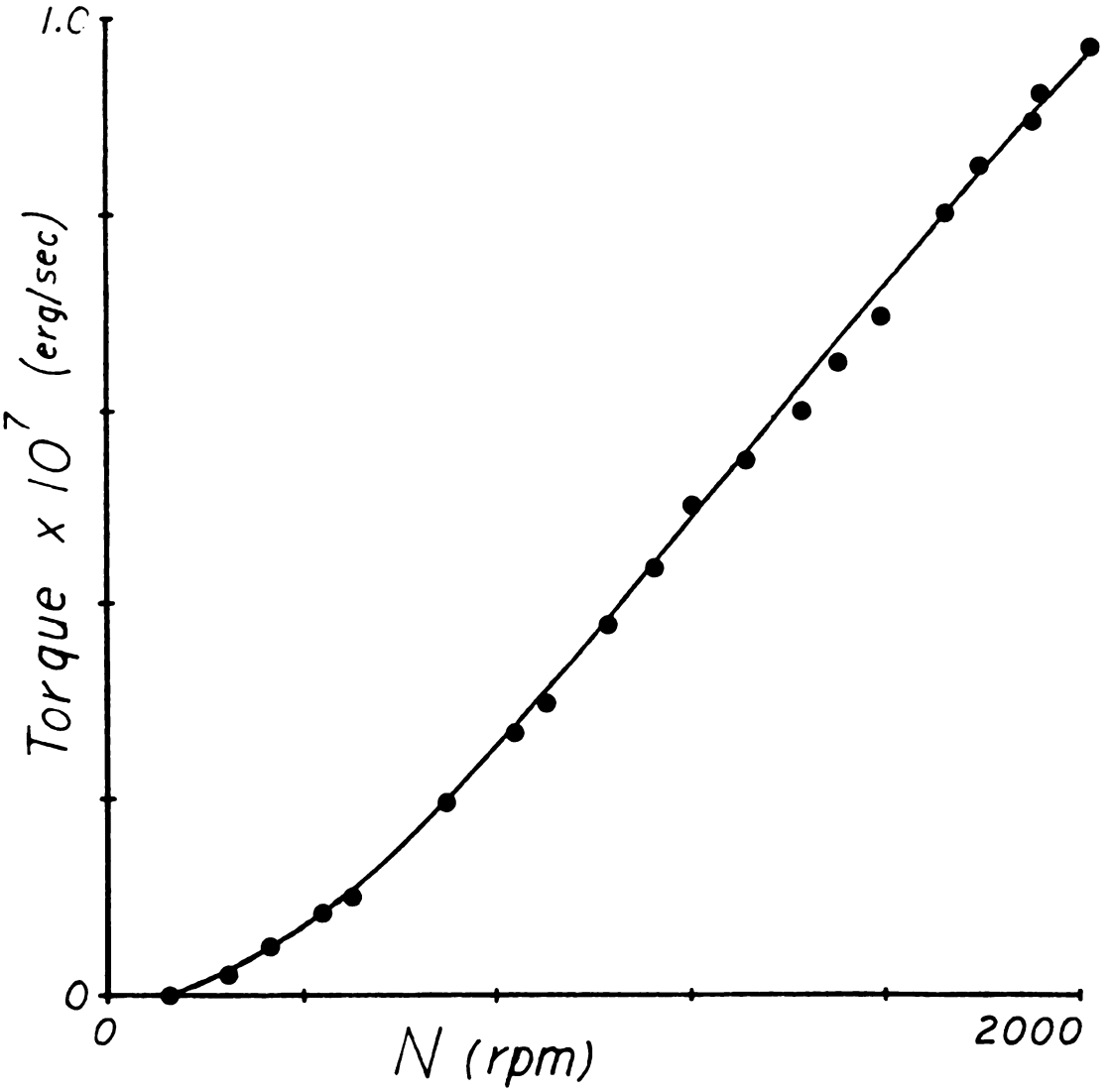

FIGURE 7. Measured Torque Versus Impeller Speed.

tend to coagulate. The hydrophobic nature of parts of the random coil are thought to be responsible for the aggregation (20).

Quantitatively, the increased activity upon shearing raised the effective initial activity by a factor of 1.02 to 1.10. Extending this analysis, roughly 2 to 10 percent of the enzyme was found to be inactivated by molecular aggregation prior to shearing. In all cases, the effect of continued shear was to reduce the activity so that the improved catalytic activity was destroyed within fifteen minutes.

THEORETICAL ANALYSIS

A. Development of Stirred Tank Rate Expressions from Couette Flow Data

The sensitivity of catalase to a discrete shear rate is a known relationship derived from the couette viscometer experiments. The rate of enzyme inactivation for a single shear rate s can be written

$$R_s\Big|_s = Ks\Big|_s a \qquad 21$$

If the fluid in a turbulent flow field is conceptualized as a continuously backmixing system of differential volumes each experiencing a specific shear rate, then it should be possible to model the sensitivity of enzymes to the turbulent shear within a stirred tank. For such a turbulent system, the degradation rate expression becomes,

$$R_t = \int K_s a F_{(s)} ds \qquad 22$$

where $F_{(s)}$ is the normalized shear rate probability density function defined by

$$\int F_{(s)} ds = 1 \qquad 23$$

Integration is over the domain of $F_{(s)}$.

Although hot-wire and laser-dopler anemometry has been used by a number of authors (18, 23) to partially characterize the profiles of fluctuating velocities in stirred

tanks, the form of the shear distribution function is in general not known. In this work, several hypothetical shear distribution functions are proposed. The rate expressions so generated are compared to the actual degradation rate determined by experiment. It is hoped that the results will not only provide a useful method for predicting activity loss for industrially applicable stirred tank enzyme reactors, but also provide some insight into an important area of turbulence research.

B. Several Distribution Functions and Resultant Rate Expressions

1. Linear Distribution

From the definition of the distribution function given in equation 23, one finds that the units of F must be time or the reciprocal of shear rate. A simple linear distribution of shear could be modeled by

$$F_{(s)} = As + C \qquad 24$$

where A and C are unknown and the shear rate varies from zero to some maximum permissible value s_{max}.

One of the constants can be eliminated by using the definition equation,

$$\int_0^{s_{max}} F_{(s)} ds = 1 \qquad 25$$

substituting equation 24 gives

$$\int_0^{s_{max}} (As + C)\, ds = 1 \qquad 26$$

where $C = \frac{B}{s_{max}}$

Integration and evaluation of limits results in the expression

$$1 = \frac{A}{2} s_{max}^2 + B \qquad 27$$

where B is an unknown constant. Now,

$$A = \frac{2(1-B)}{s_{max}^2} \quad \text{and} \quad C = \frac{B}{s_{max}} \qquad 28$$

By substituting these expressions for A and C into equation 24, the distribution function takes the form,

$$F_{(s)} = \frac{2(1-B)}{s_{max}^2} s + \frac{B}{s_{max}} \qquad 29$$

Since this model is generalized, various values for B can be selected to alter the shape of the distribution function as is shown in Figure 8a. This function can now be used to satisfy the stirred tank degradation reaction rate equation.

$$R_t = \int_0^{s_{max}} Zas\{\frac{2(1-B)}{s_{max}} s + \frac{B}{s_{max}}\} ds \qquad 30$$

The proportionality Z and the enzyme activity are assumed to be independent of s. The continuous backmixing of the tank contents prevents the activity of a differential

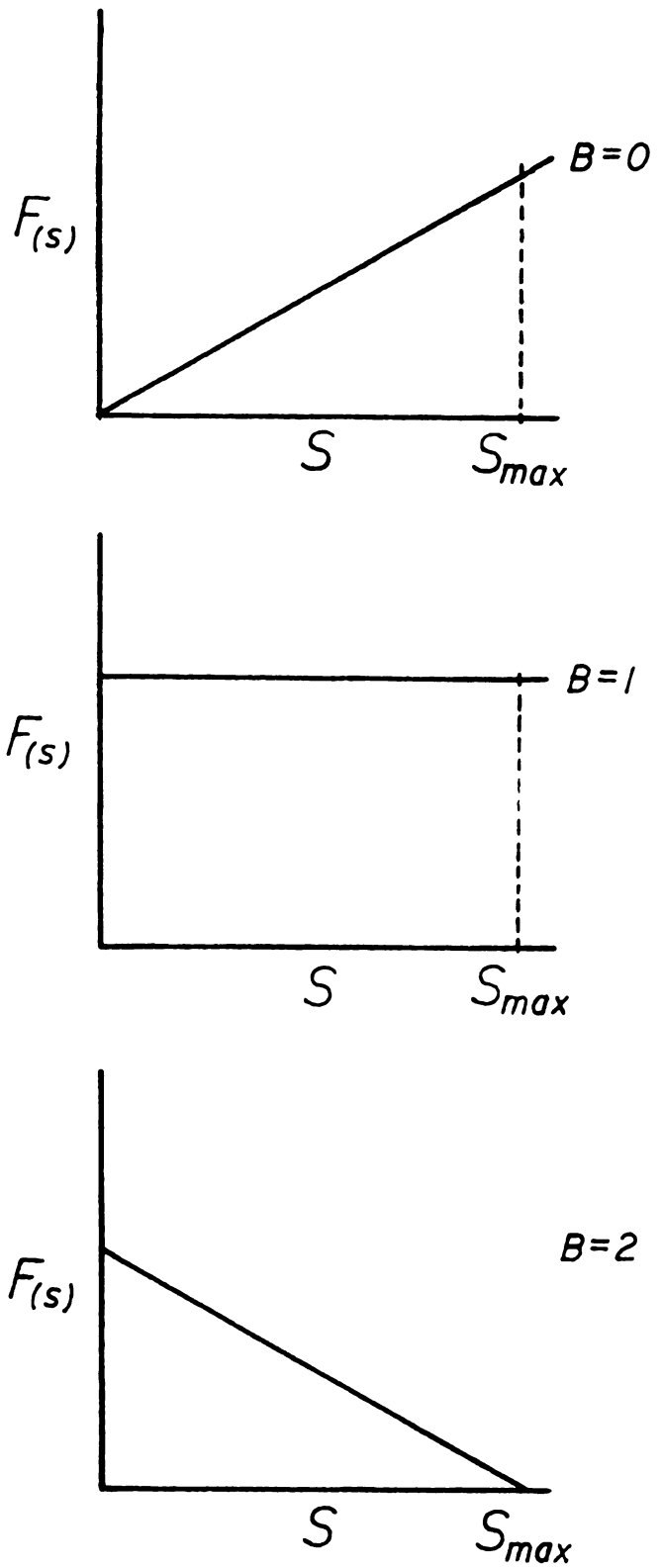

FIGURE 8a. The Linear Distribution Function for B = 0, 1, 2.

eddy from depending upon the rate of shear it experiences. After integration and evaluation of limits, the rate expression becomes

$$R_t = \left(\frac{4-B}{6}\right) Z a s_{max} \qquad 31$$

Although the value s_{max} is not measured directly it can be evaluated by using the equation of motion for cylindrical coordinates to get the dissipation of energy term (4).

$$\frac{dP}{dV} = \mu s^2 \qquad 32$$

Again, the definition of the distribution function can be used to show

$$Fds = \frac{dv}{V} \qquad 33$$

so that

$$dP = \mu s^2 VFds \qquad 34$$

or

$$\int_0^P dP = \mu V \int_0^{s_{max}} s^2 Fds \qquad 35$$

substitution of equation 29 and solution of the integral gives

$$s_{max}^2 = \frac{6}{3-B} \frac{P}{\mu V} \qquad 36$$

Equations 31 and 36 can be combined to give,

$$R_t = \frac{4-B}{\sqrt{6}\ \sqrt{3-B}}\ \frac{Z}{\mu^{\frac{1}{2}}}\left(\frac{P}{V}\right)^{\frac{1}{2}}\ a \qquad 37$$

where the degradation rate constant K_t is given by

$$K_t = \frac{4-B}{\sqrt{6}\ \sqrt{3-B}}\ \frac{Z}{\mu^{\frac{1}{2}}}\left(\frac{P}{V}\right)^{\frac{1}{2}} \qquad 38$$

2. Gaussian Distribution

Since shear rates can be both positive and negative, the distribution of shear rate in a turbulent system may be modeled as random with a true average at zero shear rate. The normal probability density function is then

$$F_{(s)} = \frac{1}{\sqrt{\langle s^2\rangle}\ \sqrt{2\pi}}\ \exp\left\{\frac{-s^2}{2\langle s^2\rangle}\right\} \qquad 39$$

where $\langle s^2\rangle$ is the second moment or variance of s. Notice that no constants must be evaluated and that the domain of F is from negitive infinity to positive infinity, Figure 8b.

This function can be substituted into equation 3 to give

$$R_t = \int_{-\infty}^{\infty} Zas\ \frac{1}{\sqrt{\langle s^2\rangle}\ \sqrt{2\pi}}\ \exp\left\{\frac{-s^2}{2\langle s^2\rangle}\right\}\ ds \qquad 40$$

Removing constant terms from the integral and solving results in a rate expression in terms of the second moment

$$R_t = \frac{2}{\sqrt{2\pi}}\ \langle s^2\rangle^{\frac{1}{2}}\ Za \qquad 41$$

Since by definition

$$\langle s^2\rangle = \int s^2 F ds \qquad 42$$

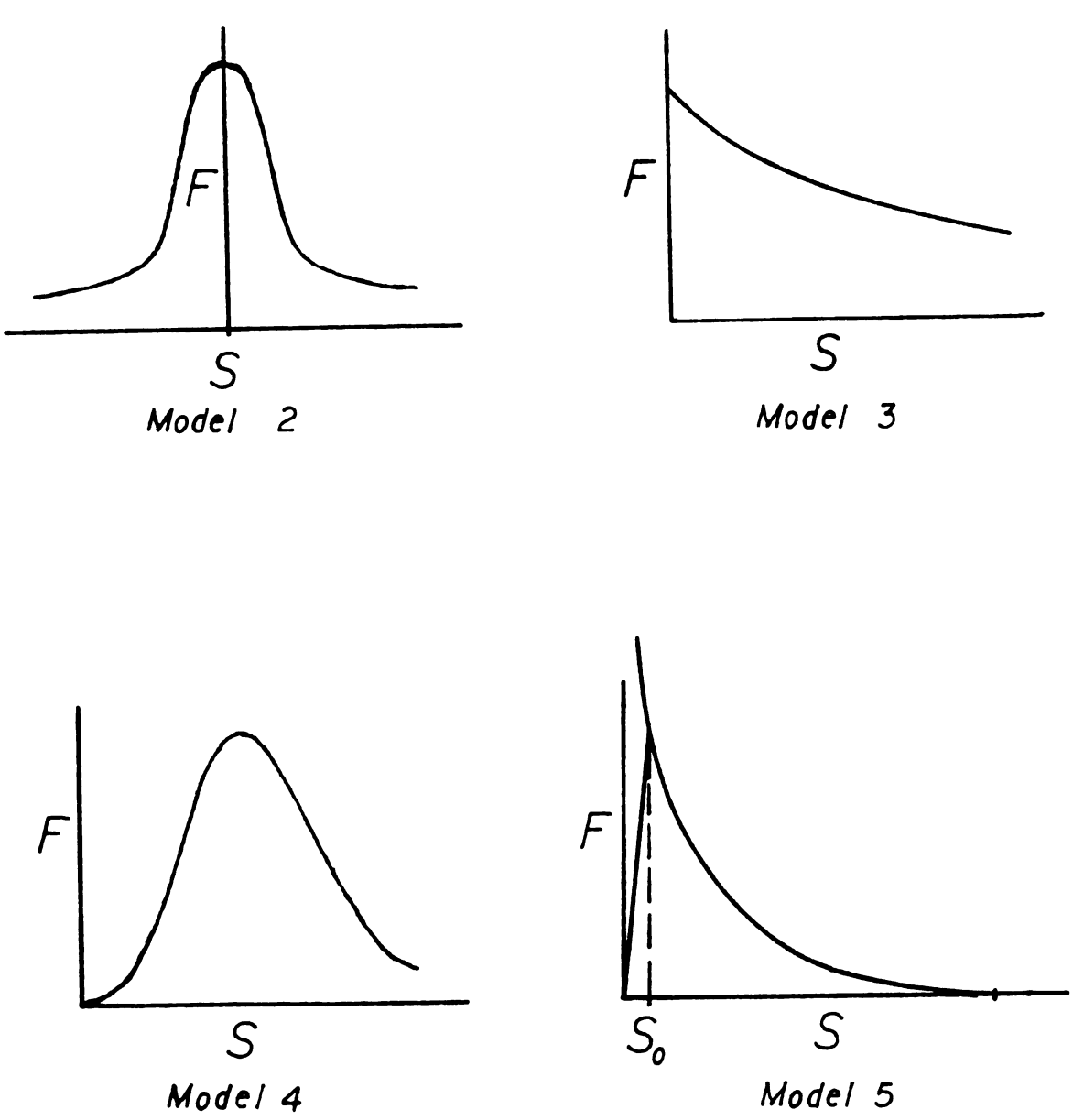

FIGURE 8b. A Schematic Representation of Models 2 Through 5.

one can show by equation 32 that for any arbitrary distribution function

$$\langle s^2 \rangle = \frac{P}{\mu V} \qquad 43$$

This result is substituted into equation 41 to give the rate expression

$$R_t = \frac{2}{\sqrt{2\pi}} \frac{Z}{\mu^{\frac{1}{2}}} \left(\frac{P}{V}\right)^{\frac{1}{2}} a \qquad 44$$

so that

$$K_t = \frac{2}{\sqrt{2\pi}} \frac{Z}{\mu^{\frac{1}{2}}} \left(\frac{P}{V}\right)^{\frac{1}{2}} \qquad 45$$

Since there is no artificial end point for this distribution (e.g. s_{max}), then the resulting rate expression has no adjustable parameters.

3. Exponential Form

A simple and intuitive distribution function predicts that low shears will be more abundant, and that the probability distribution decays exponentially with the magnitude of s. This model is shown in Figure 8b and can be written

$$F_{(s)} = ce^{-cs} \qquad 46$$

The constant can be evaluated by finding the first moment (or mean) of shear rate.

$$\langle s \rangle = \int_0^\infty s^2 F ds \qquad 47$$

By substituting equation 46 the mean shear can be found in terms of c.

$$\langle s \rangle = \frac{1}{c} \qquad 48$$

The distribution function then becomes

$$F_{(s)} = \frac{1}{\langle s \rangle} \exp(-\frac{s}{\langle s \rangle}) \qquad 49$$

Substituting F into equation 3, the resulting rate expression is given in terms of the mean shear rate.

$$R_t = \Gamma(2)\langle s \rangle Za \qquad 50$$

Once again, the energy dissipation expression can be used to determine <s> in terms of P/V.

$$\frac{P}{\mu V} = \langle s^2 \rangle = \int s^2 F_{(s)} ds \qquad 51$$

Solving the integral gives

$$\langle s^2 \rangle = 2\langle s \rangle^2 \qquad 52$$

By substituting equation 52 into the rate expression from equation 50, one can show that

$$R_t = \frac{\Gamma(2)}{\sqrt{2}} \frac{Z}{\mu^{\frac{1}{2}}} (\frac{P}{V})^{\frac{1}{2}} a \qquad 53$$

4. Log-Normal Form

The flow pattern in a stirred tank has been fairly well established (10). While basically radial in nature, the

presence of the baffles often causes regions of relatively stagnant fluid at very low shear rates. The fraction of fluid is normally low in these stagnant pockets suggesting that the distribution function will reach a maximum at some moderate rate of shear. The following model shown in Figure 8b provides for this type of behavior.

$$F_{(s)} = C's \exp(-C's^2) \qquad 54$$

The constant can readily be determined in terms of the second moment to give a distribution function of the form

$$F_{(s)} = \frac{s}{2\langle s^2 \rangle} \exp\left(-\frac{s}{2\langle s^2 \rangle}\right) \qquad 55$$

Substitution into equation 3 and integration results in a rate expression given by

$$R_t = \frac{\sqrt{2\pi}}{4} \frac{Z}{\mu^{\frac{1}{2}}} \left(\frac{P}{V}\right)^{\frac{1}{2}} a \qquad 56$$

5. Composite Form

According to Holland and Chapman (10), the shear rate can be modeled as decaying exponentially from the center of the tank. This model can be expressed as

$$s = s_{max} \exp\left(-m\frac{r}{R}\right) \qquad 57$$

where r is the distance from the tank axis and R is the tank radius. The volume contained in some radius r is,

$$v_{(r)} = \pi r^2 \ell \qquad 58$$

where ℓ is 2r. The tank volume is,

$$V = \pi R^2 2R \tag{59}$$

The ratio of r/R can now be expressed as a function of v/V.

$$r/R = \sqrt[3]{v/V} \tag{60}$$

The constant m can now be evaluated for the tank wall condition where v/V = 1 and s is equal to some wall shear rate s_0. Solving for m gives,

$$m = -\ln\left(\frac{s_0}{s_{max}}\right) \tag{61}$$

At a specific shear rate (or radius) v is given by

$$v_{(r)} = V \frac{-\ln\left(\frac{s}{s_{max}}\right)}{-\ln\left(\frac{s_0}{s_{max}}\right)} \tag{62}$$

Using equation 33, one can write

$$F = \frac{1}{V}\frac{dv}{ds} \tag{63}$$

where the differential change in volume with respect to shear rate is,

$$\frac{dv}{ds} = \frac{d}{ds}\left\{-\frac{\ln\left(\frac{s}{s_{max}}\right)}{\ln\left(\frac{s_{max}}{s_0}\right)}\right\}V \tag{64}$$

or

$$\frac{dv}{ds} = 3V\frac{\left\{\ln\left(\frac{s_{max}}{s}\right)\right\}^2}{\left\{\ln\left(\frac{s_{max}}{s_0}\right)\right\}^3}\left(\frac{-s}{s_{max}}\frac{s_{max}}{s^2}\right) \tag{65}$$

so the distribution function becomes,

$$F_{(s)} = \frac{3}{\{\ln(\frac{s_{max}}{s_0})\}^3} \frac{\{-\ln(\frac{s}{s_{max}})\}^2}{s} \qquad 66$$

$$s_0 \leq s \leq s_{max}$$

Since baffles are used in this tank s_o does not represent the true minimum shear rate found in the tank. As mentioned before, the use of baffles results in some nearly stagnant pockets of fluid which will exhibit a shear rate lower than the wall condition. This condition is handled by a linear model as shown in Figure 8b. This gives

$$F_{(s)} = \frac{3}{s_0^2} \frac{s}{\ln(\frac{s_{max}}{s_0})} \qquad 67$$

$$0 \leq s \leq s_0$$

The rate expression is obtained by substituting equations 66 and 67 into equation 3. The rate expression is in terms of s_o.

$$R_t = \frac{Zas_0}{\ln(\frac{s_{max}}{s_0})} \{ \frac{6(\frac{s_{max}}{s_0} + 1)}{\{\ln(\frac{s_{max}}{s_0})\}^2} + \frac{2}{\ln(\frac{s_{max}}{s_0})} - 2 \} \qquad 68$$

Using the energy dissipation equation as before, s_o can be evaluated in terms of $(P/V)^{\frac{1}{2}}$ to give

$$R_t = \frac{8}{3} \frac{\dfrac{3\left(\dfrac{s_{max}}{s_0} + 1\right)}{\{\ln\left(\dfrac{s_{max}}{s}\right)\}^2} + \dfrac{1}{\ln\left(\dfrac{s_{max}}{s_0}\right)} - 1}{\dfrac{\left(\dfrac{s_{max}}{s_0}\right)^2 - 1}{\{\ln\left(\dfrac{s_{max}}{s_0}\right)\}^2} - \dfrac{2}{\ln\left(\dfrac{s_{max}}{s_0}\right)} - 1} \frac{Z}{\mu^{\frac{1}{2}}} \left(\frac{P}{V}\right)^{\frac{1}{2}} a \qquad 69$$

The elaborate form of the constant factor is due to the integration which needs to be done in two steps; from s equals zero to s_0 and from s equals s_0 to s_{max}. This result differs from the other models because of the unknown parameter s_0. The quanity s_{max}/s_0 can be found by comparison with the experimentally determined stirred tank rate expression.

Table 5 summarizes the theoretical developments giving each shear distribution function and the value of the numerical value G. Notice that the predicted rate expression is sensitive to the form of the shear distribution function.

For the isolated case where the degradation rate is second order with respect to shear, it can be shown that the rate expression is independent of the form of F. Given

$$R_s = Zas^2 \qquad 70$$

then, for any function F,

$$R_t = \int R_s F ds = \int Zas^2 F ds = Za\int s^2 F ds \qquad 71$$

or

Table 5. Summary of each model and their results.

Model	Form of F	Value of G
1, B=0	$\frac{2(1-B)}{s_{max}} s + \frac{B}{s_{max}}$	0.943
1, B=1	same	0.866
1, B=2	same	0.816
2	$\frac{1}{\sqrt{<s^2>}\sqrt{s\pi}} \exp\{\frac{-s^2}{2<s^2>}\}$	0.799
3	$\frac{1}{<s>} \exp\{-\frac{s}{<s>}\}$	0.707
4	$\frac{s}{2<s^2>} \exp\{-\frac{s^2}{2<s^2>}\}$	0.627
5	$\frac{3}{\{\ln(\frac{s_{max}}{s_0})\}^3} \frac{\{-\ln(\frac{s}{s_{max}})\}^2}{s}$ $s_0 \leq s \leq s_{max}$ $\frac{3}{s_0^2} \frac{s}{\ln(\frac{s_{max}}{s_0})}$ $0 \leq s \leq s_0$	0.256
Experimental		0.256

$$R_t = Za\langle s^2 \rangle \qquad 72$$

Recall that for any distribution function

$$\langle s^2 \rangle = \frac{P}{\mu V} \qquad 43$$

so that the rate expression becomes,

$$R_t = \frac{ZP}{\mu V} a \qquad 73$$

Hence, for a second order dependence on the shear, the predicted rate of degradation in the tank is not dependent upon the form of the shear distribution function. This would seem to imply that the enzyme degradation kinetics as determined by the couette experiments can be extrapolated to <u>any</u> turbulent flow system. Only the rate of energy dissipation and viscosity of the system would be required to characterize the rate of enzyme activity loss.

DISCUSSION

A. Comparison of Mathematical Models and Experimental Results

Each of the models presented above results in an overall enzyme degradation reaction rate expression for the stirred tank which has the form,

$$R_t = K_t a \qquad 74$$

where

$$K_t = G \frac{Z}{\mu^{\frac{1}{2}}} \left(\frac{P}{V}\right)^{\frac{1}{2}} \qquad 75$$

The models vary only in the dimensionless constant of proportionality G.

Recall that the viscosity μ is known, the value of Z is determined experimentally, and the power input is obtained from torque data. The value of G can then be calculated from the experimental results by plotting K_t vs. the quanity $\frac{Z}{\mu^{\frac{1}{2}}} \left(\frac{P}{V}\right)^{\frac{1}{2}}$. Figure 9 shows this plot for the experimental results and each of the proposed models. In general the predicted rates of activity loss are somewhat high. As expected, those models which are more carefully developed result in a progressively better fit to the data.

Model 5, which contains an adjustable parameter, fits the data well when s_{max}/s_o is 37.33. The implication is that a shear rate of roughly 2.7 percent of the maximum will be most commonly found. An important result of this study is

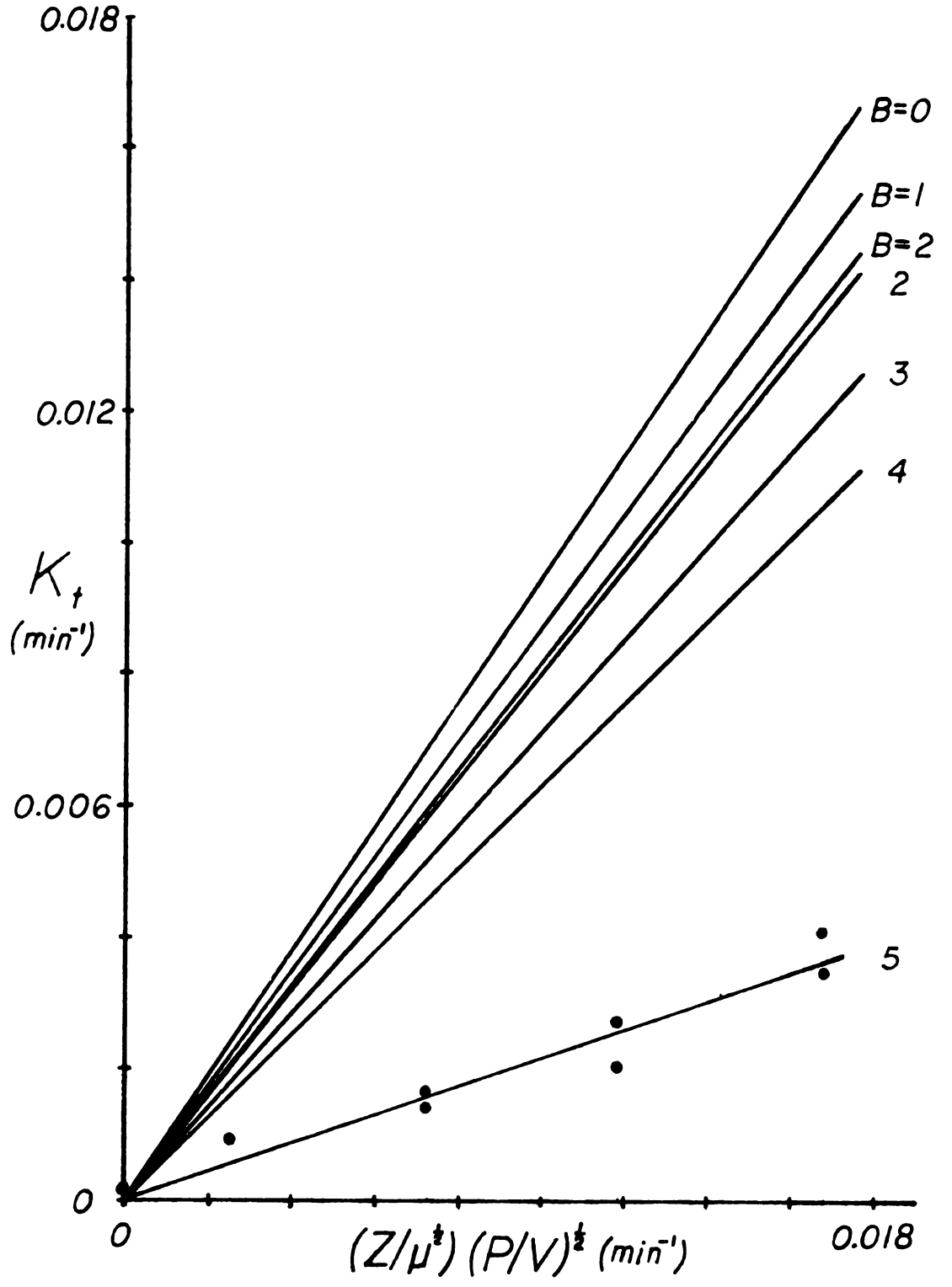

FIGURE 9. K_t vs. $(Z/\mu^{\frac{1}{2}})(P/V)^{\frac{1}{2}}$ for the models and for the stirred tank data.

that predicted reaction rates using couette data are indeed sensitive to the distribution of shear rates in the tank.

B. Possible Degradation Mechanisms

A number of scenarios have been developed to describe the modification of protein structure or function at the molecular level. Much of the work is isolated and provides no common basis from which a generally accepted mechanism of shear modification can be developed.

Early research by Joly and Barbu (1) examined low concentrations of horse serum albumin and tobacco mosaic virus. They found that for low shears in a couette viscometer, there was an increase in the effective particle length as measured by flow birefringence. According to the authors, at the molecular level shearing increases the collision frequency of the particles, promoting aggregation and increasing apparent length. This phenomena was explained by the collision coagulation theory of Smoluchowski (17) modified to account for varying interaction strengths between particles. One may infer that the loss of enzyme activity could be caused by this shear-induced aggregation effect. At higher shears (above 2000 sec^{-1}), the aggregates were ruptured but the authors did not investigate the further action of shear on the particles.

There is evidence in the medical literature for plasma protein denaturation in flow through extracorporeal devices.

The strong intermolecular forces at blood-gas interfaces have been shown to cause protein denaturation (22). This group claims that the presence of blood-solid interfaces may also cause damage to blood proteins. Studies of flow induced erythrocyte damage show that near solid boundaries, shear stresses of one Pascal or less can cause erythrocyte lysis (12). In the absence of walls, the critical shear stress for lysis has been estimated to be 6000 Pascals in liquid-into-liquid jet experiments (5). The validity of this comparison must be questioned in light of the great difference in the method of applied stress.

Within the last ten years, considerable work has been done with specific enzymes which have been fairly well characterized. The results of much of this work imply that hydrodynamic forces are not directly causative of protein modification but act to reduce somewhat the activation energy for the degradation reaction (20). The energy of the turbulent shear causes tension in some bonds making them more labile and resulting in a less stable protein structure.

C. Suggestions for Further Work

The structure of the turbulence within a stirred tank is not well known. A better understanding of this structure would provide a valuable tool for the modeling of hydrodynamically related phenomena. The structural modification of biological compounds in a stirred tank is ultimately

caused by the dissipation of energy. It is known that most of the kinetic energy of an agitated fluid is dissipated at the smallest scales of turbulence, and that extensional flows may become an important or even the predominant mechanism of energy dissipation.

In order to more accurately predict activity losses and describe protein deactivation at the molecular level, it may become necessary to understand the sensitivity of enzymes to extensional flow as well as shear flow. Although devices have been designed which produce a pure elongational flow (4), they may be difficult to model as a continuous flow system. The couette apparatus can be used to generate Taylor vortices which contain both shear and extensional flows but are readily modeled.

CONCLUSION

The primary goal of this thesis is to provide a reliable method for the prediction of the rates of enzyme activity loss in a turbulent system of practical value, e.g. a stirred tank. First the response of enzyme activity to a pure shear field is determined experimentally in a couette viscometer. Then, if the stirred tank turbulence is modeled as a collection of differential packets each experiencing a distinct shear, the couette kinetic data can be used to predict the total rate of activity loss.

Turbulence research has as yet not established the distribution of shears in a complicated system like a stirred tank. Consequently, various hypothetical functions are proposed to characterize the shear distribution. In each case, the form of the predicted rate expression reduces to,

$$R_t = G \frac{Z}{\mu^{\frac{1}{2}}} \left(\frac{P}{V}\right)^{\frac{1}{2}} a \qquad 76$$

where the rate constant is given by

$$K_t = G \frac{Z}{\mu^{\frac{1}{2}}} \left(\frac{P}{V}\right)^{\frac{1}{2}} \qquad 77$$

The models differ only in the form and value of the constant G.

In reviewing the forms of the distribution functions diagrammed in Figure 8, one may conclude that the shear

probability function reaches a maximum at some intermediate shear rate. For the tank used here, a shear rate equal to 2.7 percent of the maximum was predicted to be most common. Although this model seems to provide an adequate description of shear for enzyme degradation, it would be unwise to assume an a priori knowledge of the shear distribution for use in other shear sensitive operations (e.g., mixing).

Rate data were taken in two geometrically similar tanks. The resultant rate expressions are functions of enzyme sensitivity to shear, viscosity, and power per volume. Shear sensitivity varies with temperature and between species. These results seem to indicate that a useful scale-up criterion can be based on the power input. This would eliminate the necessity of first predetermining the degradation characteristics in a coaxial device for each tank volune change.

A transient enhancement of activity was noticed for both the viscometer and the stirred tank. It is believed that aggregates of enzyme molecules are broken up by the shear force resulting in an increase in the initial activity. Increases of two to ten percent were found.

Data taken in a smaller, geometrically similar tank, support the findings in this work. In both tanks, the rate of enzyme degradation has been shown to be proportional to the square root of power per volume. It is suggested that this observation can be used as a criterion for scaling to other sizes of stirred tanks.

APPENDICES

APPENDIX A

Viscometer and Tank Dimensions

APPENDIX A

Viscometer Dimensions (cm)

Inner diameter of outer cylinder	11.8491
Outer diameter of inner cylinder	11.6891
Outer cylinder height	20.10
Inner cylinder height	25.6
Gap width	0.08
Gap volume	70 cm

Stirred Tank Dimensions (cm)

Tank diameter	21.0
Fluid depth	21.0
Baffle width	1.75
Impeller width	7.00
Blade width	1.40
Blade height	1.12
Impeller height from bottom	7.00
Shaft diameter	1.61
Tank volume	6670 cm

APPENDIX B

Tabulated Data

APPENDIX B

Tabulated Data

Torque vs. Impeller Speed

Mass (gm)	N	Torque $X10^{-7}$ erg
0	125	-0-
10	175	0.1
20	225	0.2
30	270	0.3
50	325	0.5
80	440	0.8
100	495	1.0
120	545	1.2
170	655	1.7
200	700	2.0
220	750	2.2
270	830	2.7
300	900	3.0
320	925	3.2
350	975	3.5
370	1020	3.7
395	1070	3.9
455	1150	4.6
475	1190	4.7
500	1210	5.0
550	1315	5.5
600	1430	6.0
650	1500	6.5
700	1590	7.0
750	1650	7.5
800	1725	8.0
850	1790	8.5
895	1900	8.9
925	1920	9.2
975	2020	9.7

Viscometer N = 0 rpm s = 0 sec^{-1} K_v = .001027 min^{-1}

Assay	t	θ	k'
1	12:15	0	.019263
2	12:19	4	.02129
3	12:23	8	.02085
4	12:27	12	.02222
5	12:30	15	.02091
6	12:33	18	.02108
7	1:15	60	.01984
8	1:25	70	.02001
9	1:35	80	.01948
10	2:40	145	.01833
11	2:43	148	.01659
12	2:46	151	.01775
13	2:49	154	.01770
14	3:35	200	.01698
15	3:38	203	.01782
16	3:42	207	.01781
17	3:45	210	.01679

Viscometer N = 83.3 rpm s = 643.0 sec^{-1} K_v = .00131 min^{-1}

Assay	t	Θ	k'
1	1:37	-13	.022546
2	1:41	- 9	.019823
3	1:44	- 6	.020030
4	1:50	0	.019360
5	1:55	5	.019904
6	2:00	10	.019945
7	2:10	20	.018998
8	2:20	30	.018337
9	2:50	60	.017362
10	3:20	90	-
11	3:50	120	.016387
12	4:20	150	.015314
13	4:55	185	.015316
14	5:20	210	.014877
15	5:25	215	.014950
16	5:30	220	.015124
17	5:35	225	.014760

Viscometer N = 166.7 rpm s = 1286 sec^{-1} K_v = .00139 min^{-1}

Assay	t	θ	k'
1	9:50	-15	.01629
2	9:54	-11	.01690
3	9:58	- 7	.01661
4	10:05	0	.01669
5	10:10	5	.01827
6	10:15	10	.01739
7	10:20	15	.01679
8	10:25	20	.01646
9	10:35	30	.01606
10	11:05	60	.01469
11	11:35	90	.01451
12	12:05	120	.01494
13	12:35	150	.01222
14	1:05	180	.01460
15	1:35	210	.01235
16	2:05	240	.01324
17	2:35	270	.01145

Viscometer N = 250 rpm s = 1929 sec^{-1} K_v = .001628 min^{-1}

Assay	t	θ	k'
1	11:10	-10	.02200
2	11:14	- 6	.02073
3	11:17	- 3	.02268
4	11:20	0	.01911
5	11:25	5	.01918
6	11:30	10	.02068
7	11:40	20	.01524
8	11:50	30	.01664
9	12:20	60	.01600
10	12:50	90	.01540
11	1:20	120	.01481
12	1:50	150	.01442
13	2:20	180	.01398
14	2:50	210	.01336
15	3:00	220	.01306
16	3:10	230	.01370
17	3:20	240	.01232

Viscometer N = 333.3 rpm s = 2572 sec^{-1} K_v = .001860 min^{-1}

Assay	t	Θ	k'
1	11:31	-	-
2	11:40	-22	.01876
3	11:44	-18	.01776
4	11:50	-12	.01762
5	11:57	- 5	.01770
6	12:02	0	.01757
7	12:07	5	.01881
8	12:12	10	.01718
9	12:17	15	.01669
10	12:22	20	.01585
11	12:32	30	-
12	12:47	45	.01638
13	1:02	60	.01556
14	1:17	75	.01446
15	1:36	94	.01449
16	1:47	105	.01486
17	2:02	120	-
18	2:17	135	.01497
19	2:32	150	.01452
20	2:42	160	.01315
21	2:52	170	.01260
22	2:57	175	.01233
23	3:02	180	.01194
24	3:07	185	.01310

Viscometer N = 500 rpm s = 3858 sec^{-1} K_v = .002227 min^{-1}

Assay	t	Θ	k'
1	9:03	-22	.02022
2	9:10	-15	.01849
3	9:13	-12	.01975
4	9:17	- 8	.02095
5	9:20	- 5	.02071
6	9:25	0	.01959
7	9:30	5	.01804
8	9:35	10	.01759
9	9:45	20	.01734
10	9:55	30	.01697
11	10:25	60	.01536
12	10:55	90	.01505
13	11:25	120	.01370
14	11:55	150	.01320
15	12:25	180	-
16	12:55	210	.01130
17	1:05	220	.01028
18	1:15	230	.01117
19	1:25	240	.01098

Stirred Tank N = 500 rpm K_t = .000947 min^{-1}

Assay	t	θ	k'
1	8:53	-17	.02014
2	8:59	-11	.02000
3	9:03	- 7	.01937
4	9:10	0	.02093
5	9:15	5	.02103
6	9:20	10	.02062
7	9:25	15	.02091
8	9:30	20	.02064
9	9:40	30	.02054
10	10:10	60	.01937
11	10:40	90	.01944
12	10:50	100	.01919
13	11:00	110	.01885
14	11:10	120	.01885
15	11:40	150	.01805
16	11:55	165	.01806
17	12:00	170	.01808
18	12:05	175	.01771
19	12:10	180	.01770

Stirred Tank N = 1000 rpm K_t = .00141 min^{-1}

Assay	Time	Θ	k'
1	8:43	-17	.00858
2	8:50	-10	.00826
3	8:56	- 4	.00779
4	9:00	0	.00880
5	9:05	5	.00881
6	9:10	10	-
7	9:15	15	.00872
8	9:30	30	.00847
9	10:00	60	.00807
10	10:30	90	.00822
11	11:00	120	.00788
12	11:30	150	.00752
13	12:00	180	.00724
14	12:30	210	.00652
15	1:00	240	.00643
16	1:30	270	.00619
17	2:00	300	.00589
18	2:30	330	.00534
19	3:00	360	.00566

Stirred Tank N = 1000 rpm K_t = .001633 min^{-1}

Assay	t	Θ	k'
1	11:10	-20	.01994
2	11:15	-15	.01981
3	11:19	- 9	.01992
4	11:30	0	.01988
5	11:35	5	.02078
6	11:40	10	.01919
7	11:45	15	.01942
8	12:00	30	.01946
9	12:30	60	.01805
10	1:00	90	.01773
11	1:30	120	.01665
12	2:00	150	.01564
13	2:20	170	.01526
14	2:25	175	.01503
15	2:30	180	.01523

Stirred Tank N = 1500 rpm K_t = .001983 min^{-1}

Assay	t	Θ	k'
1	9:30	-80	.01736
2	10:40	-10	.01792
3	10:43	- 7	.01779
4	10:50	0	.01791
5	10:55	5	-
6	11:00	10	.02212
7	11:10	20	.01819
8	11:20	30	.01768
9	11:50	60	.01663
10	12:20	90	.01534
11	12:50	120	.01533
12	1:20	150	.01404
13	1:50	180	.01313
14	2:20	210	.01293
15	2:50	240	.01286

Stirred Tank N = 1500 rpm K_t = .002643 min^{-1}

Assay	t	Θ	k'
1	9:43	-27	.01306
2	9:54	-16	.01293
3	10:00	-10	.01389
4	10:10	0	.01296
5	10:15	5	.01449
6	10:20	10	.01231
7	10:25	15	.01350
8	10:30	20	.01358
9	10:40	30	.01283
10	11:10	60	.01158
11	11:40	90	.01084
12	12:10	120	.00929
13	12:40	150	.00902
14	1:10	180	.00857
15	1:40	210	.00802
16	2:10	240	.00752

Stirred Tank N = 1750 rpm K_t = .003097 min^{-1}

Assay	t	θ	k'
1	12:40	-20	.02018
2	12:45	-15	.01986
3	12:51	- 9	.02003
4	1:00	0	.01994
5	1:05	5	.02117
6	1:10	10	.01935
7	1:15	15	.01837
8	1:30	30	.01815
9	2:00	60	.01597
10	2:30	90	.01513
11	3:00	120	.01456
12	3:30	150	.01260
13	3:45	165	.01167
14	3:50	170	.01177
15	3:55	175	.01200
16	4:00	180	.01141

Stirred Tank N = 2000 rpm K_t = .003097 min^{-1}

Assay	t	θ	k'
1	8:50	-20	.01876
2	8:56	-14	.01940
3	9:00	-10	.02004
4	9:03	- 7	.01928
5	9:06	- 4	.01904
6	9:10	0	.01895
7	9:15	5	.02039
8	9:20	10	.01902
9	9:30	20	.01788
10	9:40	30	.01796
11	10:10	60	.01478
12	10:40	90	.01519
13	11:10	120	.01360
14	11:40	150	.01078
15	11:50	160	.00962
16	12:00	170	.00969
17	12:10	180	.01024

Stirred Tank N = 2000 rpm K_t = .003439 min^{-1}

Assay	t	θ	k'
1	1:02	-13	.02138
2	1:05	-10	.02084
3	1:09	- 6	.02098
4	1:15	0	.02073
5	1:20	5	.02250
6	1:25	10	.02141
7	1:35	20	.02010
8	1:45	30	.01981
9	2:15	60	.01780
10	2:45	90	.01737
11	3:15	120	.01477
12	3:45	150	.01206
13	4:15	180	.01163
14	4:25	190	.01076
15	4:35	200	.01159
16	4:45	210	.01166

BIBLIOGRAPHY

BIBIOGRAPHY

1. Barba E. and Joly M. Bull, Soc. Chem. Biol., 32 116 (1950).

2. Barman, T., Enzyme Handbook, Vol. 1, Springer, New York (1969).

3. Beck, C., Ph.D. Dissertation, Michigan State University, E. Lansing, 1979.

4. Bird, R. B., Stewart, W. E., and Lightfoot, E. N., Transport Phenomena, Wiley, New York (1960).

5. Blackshear, P. L., Dorman, F. D., Steinback, J. H., Mayback, E. J., Singh, A., and Collingham, R. E., Trans. Am. Soc. Art. Int. Org. 12 113 (1966).

6. Bowski, L. and Ryu, D. Y., Biotechnol. & Bioeng., Vol. XVI, 1974.

7. Charm, S. E., and Wong, B. L., Vol. XII, 1103 (1970).

8. Charm, S. E., and Wong, B. L., Science, 170 466 (1970).

9. Charm, S. E., and Wong, B. L., Biorheology, July 1975.

10. Holland, F. A., and Chapman, F. S., Liquid Mixing in Stirred Tanks, Reinhold, N.Y. (1960).

11. Lehninger, A. L., Biochemistry, Worth, New York, 1975.

12. Levereh, L. B., Hellums, J. D., Alfrey, C. P., and Lynch, E. C., Biophysical J., 12 257 (1972).

13. Maehly, A. C. and Chance, B., Methods of Biochemical Analysis, Vol. I, 1954.

14. Regan, D. L., Dunhill, P., Lilly, M. D., Biotechnol. & Bioeng., Vol. XVI, 333-343 (1974).

15. Sadana, A., Biotechnol. & Bioeng., Vol. XX, 781-797 (1978).

16. Skinner, K. J., Chemical & Engineering News, August 1975, 22-41.

17. Smoluchowski, M., Z. Physik Chem., 92, 129 (1918).

18. Tatterson, G. B., Heibel, J. T., and Brodkey, R. S., Ind. Eng. Chem. Fundam, 19, 175-180 (1980).

19. Tirrell, M., and Middleman, S., Biotechnol. & Bioeng., Vol. XVII, 1975.

20. Tirrell, M., Ph.D. Dissertation, University of Massachusetts, 1977.

21. Tirrell, M., and Middleman, S., Biotechnol. & Bioeng., Vol. II, 1978.

22. Wallace, H. W., Liquori, E. M., Stein, T. P., and Brooks, H., Trans. Am. Soc. Art. Int. Org., 21 450 (1975).

23. Yuu, S., and Oda, T., Chem. Eng. J., 20, 35-42 (1980).